10.2 ON QUANTIFYING WAVES AND TURBULENCE CONTRIBUTIONS TO MOMENTUM AND BUOYANCY TRANSPORT IN KATABATIC FLOWS

Marko Princevac* and Harindra J.S. Fernando
Arizona State University, Tempe, Arizona

Paolo Monti
Università degli Studi di Roma "La Sapienza", Roma, Italia

1. INTRODUCTION

Katabatic flows in the environment are highly turbulent, very large Reynolds Number (*Re*) flows. Their characteristic Reynolds Number based on the katabatic flow depth is on the order of $\mathrm{Re} = Uh/\nu \sim 10^7$, where *U*, *h* and ν are flow velocity, flow depth and kinematic viscosity of air, respectively (laboratory *Re* for the katabatic/gravity flow experiments rarely exceeds 10^3-10^4). For this reason, turbulent transport in katabatic flow dominates the molecular transport and it is of crucial importance to be able to properly model eddy diffusivities. Monti et al. (2002) proposed semi-empirical expressions for the eddy diffusivities of momentum

$$K_M = \frac{-\overline{u'w'}}{\partial U/\partial z}, \qquad (1)$$

and heat

$$K_H = \frac{-\overline{w'\theta'}}{d\overline{\theta}/dz}, \qquad (2)$$

in stably stratified environments as a function of the Gradient Richardson Number

$$Ri_g = \frac{\frac{g}{\overline{\theta}} \cdot \frac{\partial \overline{\theta}}{\partial z}}{\left[\left(\frac{\partial \overline{U}}{\partial z}\right)^2 + \left(\frac{\partial \overline{V}}{\partial z}\right)^2\right]}, \qquad (3)$$

where *U* and *V* are mean velocities in a plane parallel to the slope (*U* being along-slope component and *V* is perpendicular to *U*), *g* the gravitational acceleration, *z* the coordinate normal to the slope, θ the potential temperature, and primed quantities represent fluctuations. These expressions are shown in Figure 1.

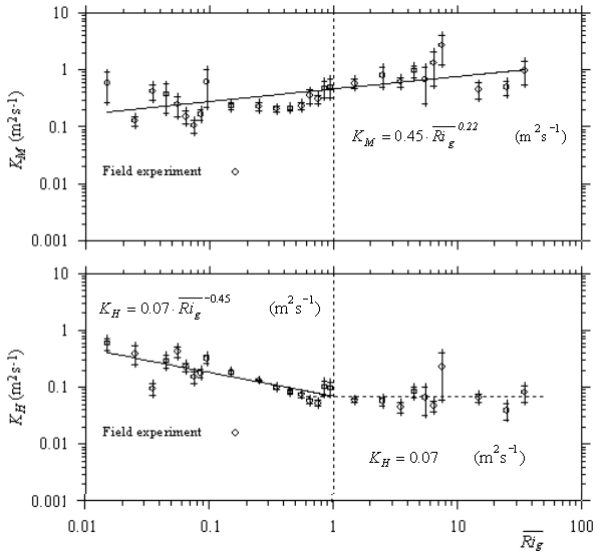

Figure 1. Dimensional eddy diffusivities of momentum and heat from Monti et al. 2002

Note that the eddy diffusivity of momentum K_M behaves differently from the eddy diffusivity of heat K_H.

Besides being highly turbulent, stably stratified katabatic flows are known to sustain intense wave activity. While turbulence is a very efficient mechanism for momentum and heat transport, linear or weakly non-linear waves are efficient in transporting the momentum but not heat. In the range of small Ri_g, the stratification effects are of lesser importance and the heat is carried by turbulent eddies at the same rate as momentum. When stratification becomes stronger (larger Ri_g), K_M becomes larger than K_H, which can be attributed to the increasing influence of buoyancy

*Corresponding author address: Marko Princevac, Arizona State University, Department for Mechanical and Aerospace Engineering, Tempe, AZ 85287-9809

that facilitates internal gravity wave activity. This wave activity efficiently transports momentum but only little (or not at all) heat.

The question that arises here is how to separate waves from turbulence? Can we, instead of "total" transports (K_M and K_H) presented in Figure 1, separately quantify transports by waves (K_{Mw} and K_{Hw}) and turbulent eddies (K_{Mt} and K_{Ht})? To address these questions we first need to look at the general characteristics of waves and turbulence. Turbulent flows are characterized by irregularity and random waves can be irregular as well. Both turbulence and non-linear waves can be diffusive. Turbulence is rotational and three-dimensional, so can be the internal waves. Turbulent flows are always dissipative while linear internal waves are essentially nondissipative, which can be a major distinction between random waves and turbulence. Turbulent motions span a continuum of scales. Turbulent energy cascades starting from large, energy-containing scale, all the way to the smallest, Kolmogorov scale $L_K = \left(\nu^3/\varepsilon\right)^{1/4}$ where turbulent dissipation occurs, and here ε is viscous dissipation rate per unit mass. This non-linear energy cascade from larger to smaller scales is absent in linear waves, and hence its spectrum is expected to be different from turbulence. Non-linear waves can have an energy cascade, but the dynamic of this cascading is expected to be different from that of turbulence due to the involvement of buoyancy effects. One way to discern internal waves is to regard all scales that deviate from Kolmogorov spectra as buoyancy dominated contributions (either linear or non-linear waves). In the co-spectra between θ' and w', the linear waves have a phase angle of 90^o.

2. DATA ANALYSIS

Wind and temperature data sampled at 10 Hz with ultrasonic anemometers during VTMX 2000 field campaign were used. The VTMX 2000 field campaign details are given in Doran et al. (2002). The same data set as in Monti et al. (2002) with four additional days, giving a total of nine nighttime periods, was used for the analysis.

Since pure turbulent diffusion is expected at smaller scales, an attempt was made to remove large fluctuating scales by assuming that transport at these scales happen mostly through the waves. In other words, it is expected that, by applying high pass filter, most of the wave transport activity is removed and turbulence transport retained.

Several different digital filters were taken into consideration. The Butterworth filter has the flattest pass-band characteristic but its transition band is wide and non-smooth. Wide transition band does not allow precise definition of the cut-off frequency. Second candidate was the Bessel filter, which gives smoothest but still wide transition band and introduces some noise in the pass-band. The Elliptical filter (also known as a Cauer response) was selected for this analysis because of its steepest transition band, although it introduces certain noise in both pass- and stop-bands. Narrow, steep transition band allowed precise definition of the cut-off frequency. Gain schematics for all three filters are shown in Figure 2 (low-pass example is given).

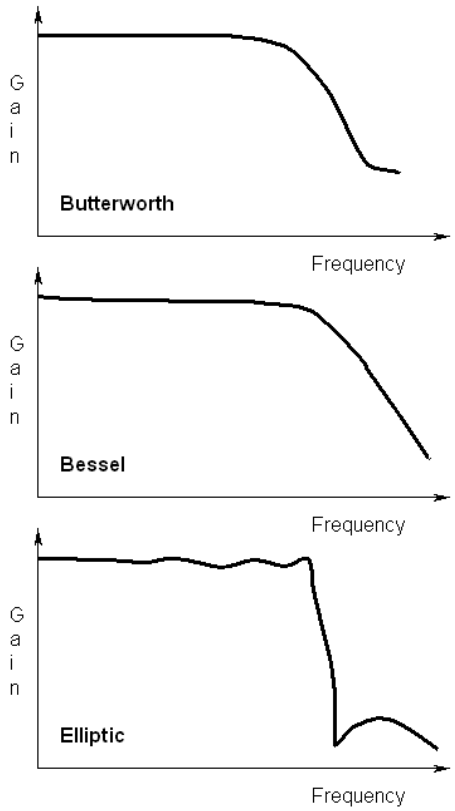

Figure 2. Characteristic gains for Butterworth, Bessel and Elliptic filter

The first parameter to be defined was the cut-off frequency. Internal gravity waves cannot have frequencies that exceed buoyancy frequency of the fluid. The observed buoyancy frequency $N = \left(g/\theta\left(d\theta/dz\right)\right)^{1/2}$ was in the range 0.05 to 0.1 rad/s, which corresponds to periods from

approximately 1 to 2 minutes. Therefore, it was decided to filter out all oscillations with periods exceeding 1 minute. Of course, by removing the *slow* oscillations, not only waves were removed but larger turbulent eddies were removed as well but these eddies are buoyancy affected, and hence can be considered as non-linear internal waves. To investigate the influence of different scales, calculations were made with different cut-off frequencies (see Section 3).

Next parameter was the filter order. Increasing filter order increases the selectivity of the filter but at the same time it will introduce more noise or unwanted signal components close to the band edge (Corral 2000). After experimenting with filter orders from one to six, the filter order three was selected as the most optimal for both, velocity and temperature data.

Simple averaging was done over one, five and fifteen minutes, and the mean value was subtracted from the instantaneous signal leaving only the fluctuating component. This remaining fluctuating component was filtered, leaving only fluctuations with frequencies higher than the cut-off frequency (quasi *wave-less signal*).

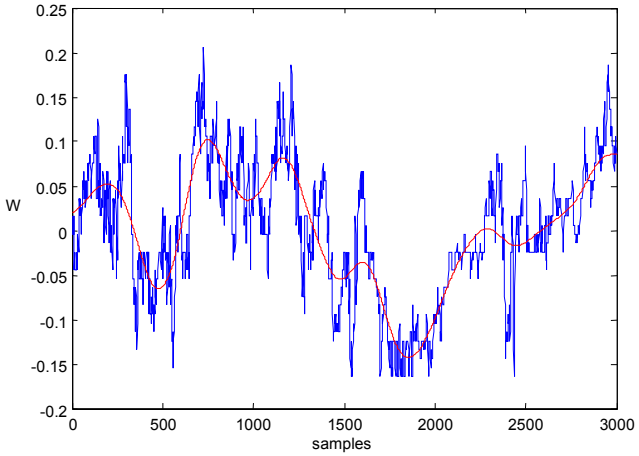

Figure 3. Five minutes of the velocity signal sampled at 10Hz with removed mean (blue line). Red line presents Elliptical filter of third order with one-minute cut-off period

There remaining fluctuations, considered to be *pure turbulent fluctuations*, were used to calculate turbulent fluxes of heat and momentum.

3. RESULTS

Turbulent fluxes calculated in this way (as described at the end of Section 2) together with vertical gradients of mean *U* velocity component and mean potential temperature θ were used to calculate the momentum (equation 1) and heat (equation 2) eddy diffusivities. Filled symbols on Figures 4 to 7 present non-filtered values, while open symbols are for filtered values. Different symbol shapes correspond to different averaging time: circle – 1 minute, square – 5 minutes and diamond – 15 minutes. In figure's legend first number followed by *m* presents averaging period in minutes and second number that appears after *fil.,* also followed by *m,* is the cut-off period in minutes. The eddy diffusivity of momentum is given in Figure 4.

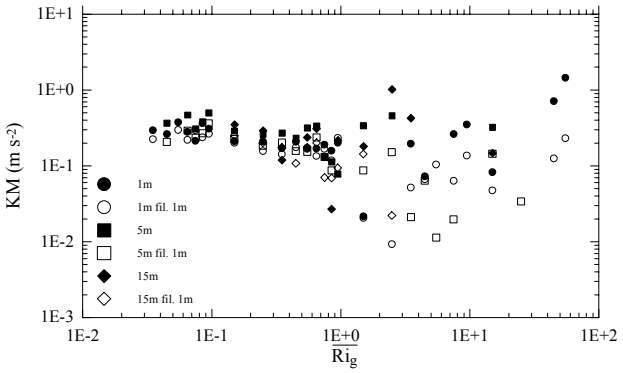

Figure 4. Dimensional eddy diffusivity of momentum

In the region with small Richardson Number ($Ri_g < 1$), there is no noticeable difference between filtered and non-filtered data. Once Ri_g becomes larger than unity, the difference becomes significant. Eddy diffusivity K_M in this region calculated using filtered data is considerably smaller. The eddy diffusivity of heat is given in Figure 5.

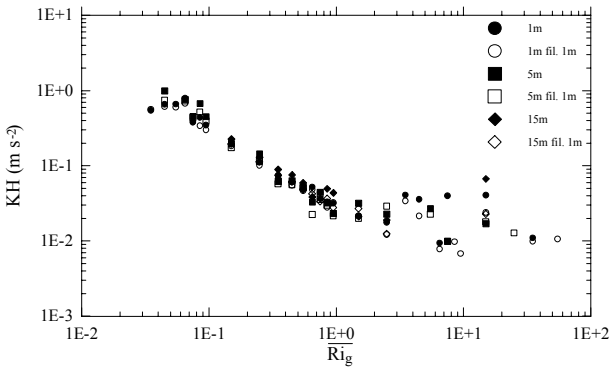

Figure 5. Dimensional eddy diffusivity of heat

Throughout the whole observed Ri_g interval, there is no glaring difference between filtered and non-filtered data for K_H. This fact suggests that large Ri_g number regimes are governed by linear gravity waves. The friction velocity $u_* = \sqrt[4]{\overline{u'w'}^2 + \overline{v'w'}^2}$ is presented in Figure 6. Five minute averages were additionally filtered with a five minutes cut-off period and fifteen minutes averages with a fifteen minutes cut-off period to investigate the influence of different scales. Small decrease in the region of $Ri_g < 1$ is noticeable due to filtering. For higher Ri_g, this decrease becomes slightly larger.

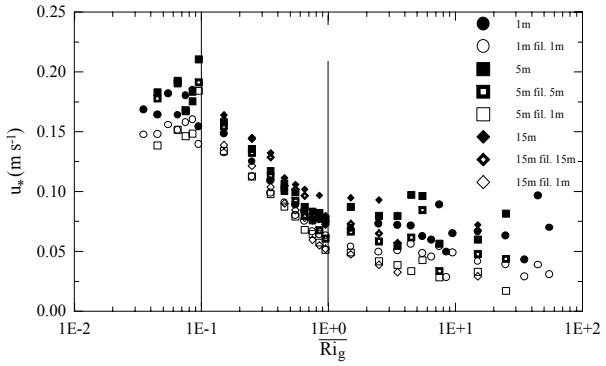

Figure 6. Friction velocity

The turbulent kinetic energy $TKE = 0.5\left(\overline{u'^2} + \overline{v'^2} + \overline{w'^2}\right)$ is given in Figure 7. Same additional cut-off frequencies are included as in the case of friction velocity plots of Figure 6.

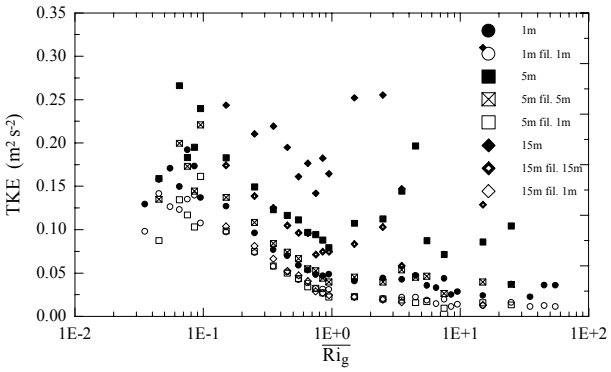

Figure 7. Turbulent kinetic energy

As expected, the removal of large scale wave-type contributions decreases the amount of kinetic energy contained therein substantially. An idea of waves to turbulent contributions can be obtained by calculating the "wave" kinetic energy TKE_{wav} by subtracting turbulent "turbulent" *TKE* from the total kinetic energy. A plot of TKE_{wav}/TKE_{tot} is shown in Figure 8. Note that in the region of small Ri_g. TKE_{wav} presents approximately 20% of the total *TKE*. For higher Ri_g, more than 50% of total kinetic energy is due to *wave* motion.

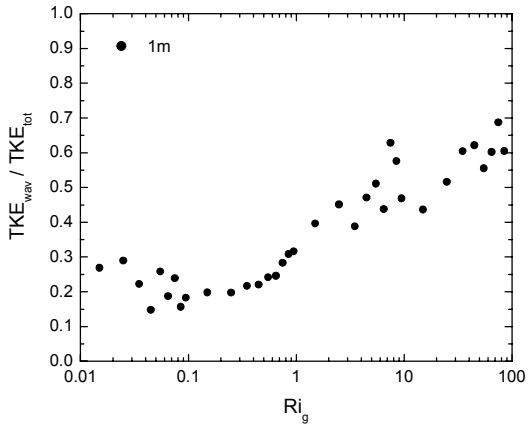

Figure 8. Contribution of wave kinetic energy to total turbulent kinetic energy

The work presented herein is the result of an ongoing investigation. At this stage, it can be concluded that the removed large oscillations (presumed to be waves) are not contributing to the heat transfer. However, they do contribute to the momentum transfer.

Acknowledgement

This research was supported by the Environmental Meteorology Program of the Department of Energy and the National Science Foundation.

References

Corral, C., 2000: Designing Elliptic Filters With Maximum Selectivity, *Energy for the Design Mind (EDN)*, Design Feature, Motorola Inc.

Doran J. C., J. D. Fast and J. Horel, 2002: The VTMX 2000 campaign, *Bull. Am. Meteorol. Soc.*, **83**(4), 537-554.

Monti, P., H.J.S. Fernando, M. Princevac, W.C. Chan, T.A. Kowalewski, and E.R. Pardyjak, 2002: Observations of Flow and Turbulence in the Nocturnal Boundary Layer over a Slope, *J. Atmos. Sci.*, **59**(17), 2513-2534.